UDC 621.373.5:621.382.3(045)

[1]**V. V. Ulansky,** D.Sc.
[2]**M.S. Fituri,** Ph.D.
[3]**I. A. Machalin,** Ph.D.

MATHEMATICAL MODELING OF VOLTAGE-CONTROLLED OSCILLATORS WITH THE COLPITTS AND CLAPP TOPOLOGY

[1,2]Al Fateh University, Tripoli, Libya, e-mail:
[1]vulanskyi@yahoo.com, [2]mfituri@hotmail.com,
[3]National Aviation University, e-mail: migor@svitonline.com

An analytical modeling is presented for the Colpitts and Clapp voltage-controlled oscillators, from which more precise equations are derived for calculation of oscillation frequency and small-signal negative resistance. Modeling is performed with taking into account a field-effect transistor parasitic capacitances. Finally, a comparison of start-up conditions is made for the Colpitts and Clapp oscillators verified by SPICE simulations. The derived equations assure a more accurate modeling, designing and implementing the Colpitts and Clapp voltage-controlled oscillators.

Introduction. *LC* oscillators are important building blocks in modern communication systems. They are widely used as voltage controlled oscillators (VCOs) in phase locked loops to up- and down-convert signals. There are several VCO topologies possible, but the most popular are the Colpitts and Clapp topologies [1 – 8]. The Colpitts and Clapp VCO design requires precise circuit modeling due to an accurate prediction of the oscillating frequency and quantitative estimation of the start-up conditions. For these reasons, the modeling of the Colpitts and Clapp VCOs is paid great attention [1 – 3], [8; 9]. At present, the small-signal models of the mentioned VCO topologies do not include transistor parasitic capacitances. These parasitic elements change the frequency response of the oscillator circuits. Consequently, the oscillation frequency, start-up condition, and other performance characteristics are affected and the real circuit operation differs from the predicted operation with ideal components. The goal of this article is to present a more accurate model for the Colpitts and Clapp VCOs.

VCO topologies. The VCOs having the Colpitts and Clapp topologies are shown in fig. 1.

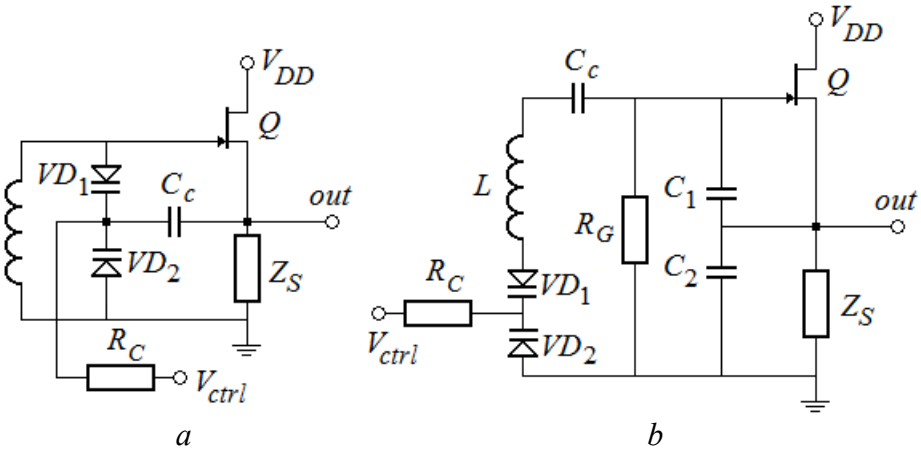

Fig. 1. VCO with the Colpitts (*a*) and Clapp (*b*) topology

The VCO`s circuit elements are here represented by the varactor diodes VD_1 and VD_2 whose capacitances are controlled by the dc control voltage V_{ctrl}, inductor L, coupling capacitor C_C, source impedance Z_S, tank capacitors C_1 and C_2, resistor R_C isolating the dc control voltage line

from the VCO tank, and resistor R_G providing zero bias voltage for the gate of transistor Q in Fig. 1(a). For a single oscillating frequency the varactor diodes can be replaced by the capacitors with capacitances C_{V1}, C_{V2} and $C_0 = C_{V1}C_{V2}/(C_{V1}+C_{V2})$ as shown in fig. 2 (a) and (b). Since the varactors are usually matched, then $C_{V1} = C_{V2} = C_V$ and $C_0 = 0{,}5C_V$.

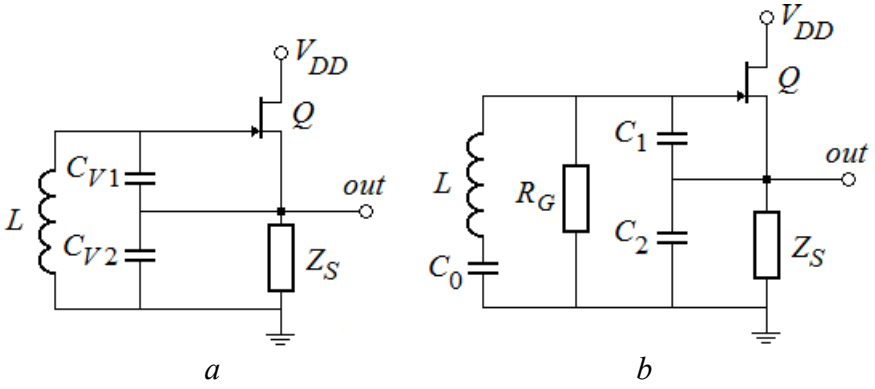

Fig. 2. Single-frequency Colpitts (a) and Clapp (b) oscillators

The junction field-effect transistor (JFET) Q in fig. 1 and fig. 2 can be replaced with any active device, such as a bipolar junction transistor (BJT), a depletion metal-oxide-semiconductor FET (MOSFET) or a metal-semiconductor FET (MESFET). As seen from fig. 2(b), the Colpitts oscillator is a special case of the Clapp oscillator in which an additional capacitor C_0 is used for controlling the frequency of oscillation. Indeed, if $C_0 \to \infty$ the circuit of fig. 2(b) becomes equivalent to the circuit of fig. 2(a).

Theoretical analysis. The Colpitts and Clapp oscillators were usually analyzed using a feedback system approach [2]. An alternative approach providing more insight into the oscillation phenomenon can be based on the concept of "negative resistance" [3], [8]. This concept is illustrated in fig. 3.

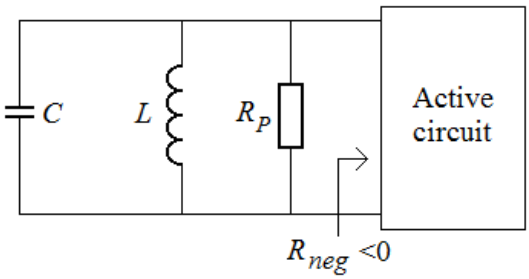

Fig. 3. *RLC* tank with negative resistance created by the oscillator active network

As seen from fig. 3, for overcoming the energy loss from a finite R_P, active circuit must form a small-signal negative resistance $(R_{neg} < 0)$, which is required to replenish the energy loss every cycle of oscillation. Thus the negative resistance can be interpreted as a source of energy. Here, R_P denotes the equivalent parallel resistance of the tank and, for oscillation start-up, it is necessary that $R_P + R_{neg} > 0$. As the oscillation amplitude increases, the amplifier will start to saturate decreasing the loop gain until it reaches unity, thereby satisfying Barckhausen criterion [2]. In the steady state the two resistances must be of equal amplitude, that is $|R_{neg}| = R_P$.

For determining a negative resistance, the input impedance of the circuit shown in fig. 2 (b) will be derived. An *ac* equivalent circuit of fig. 2 (b), ignoring the inductor L, for calculating the input impedance is shown in fig. 4, where C_{gd} is the capacitance between gate and drain, C_{gs} is the capacitance between gate and source and C_{ds} is the capacitance between drain and source.

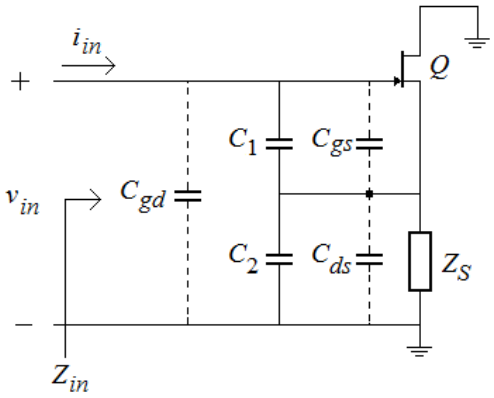

Fig. 4. An *ac* equivalent circuit of the Clapp oscillator ignoring the inductor L and capacitor C_0 and indicating the transistor terminal parasitic capacitances

Assuming $|Z_S| >> |1/j\omega(C_2 + C_{ds})|$, $r_{ds} >> |1/j\omega(C_2 + C_{ds})|$, $r_{gs} >> |1/j\omega(C_1 + C_{gs})|$, $R_G >> |1/j\omega C_{gd}|$, and replacing the transistor Q by its simplified small signal model we obtain the equivalent circuit shown in fig. 5, where r_{ds} and r_{gs} are, respectively, small-signal drain-source and gate-source resistances, g_m is the small-signal transconductance of the transistor.

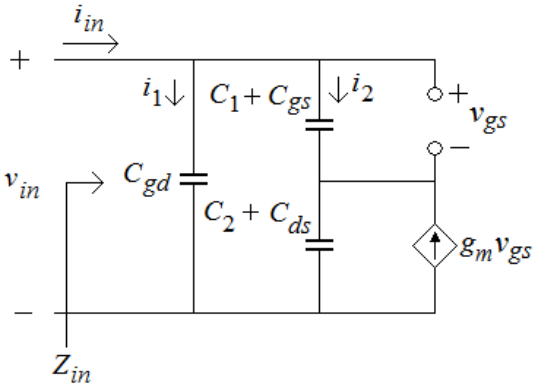

Fig. 5. Small-signal equivalent circuit of the Clapp oscillator

From fig. 5 the input impedance can be written as

$$Z_{in} = v_{in}/i_{in}. \tag{1}$$

The loop equations are given by

$$v_{in} = i_2\left(X_{C1,Cgs} + X_{C2,Cds}\right) + g_m v_{gs} X_{C2,Cds}; \tag{2}$$

$$v_{gs} = i_2 X_{C1,Cgs}, \tag{3}$$

where

$$i_2 = i_{in}\frac{X_{gd}}{X_{gd} + X_{C1,Cgs} + X_{C2,Cds}}. \tag{4}$$

Substituting i_2 from (4) into (2) and (3) gives

$$v_{in} = i_{in}\frac{X_{gd}\left(X_{C1,Cgs} + X_{C2,Cds}\right)}{X_{gd} + X_{C1,Cgs} + X_{C2,Cds}} + g_m v_{gs} X_{C2,Cds}; \tag{5}$$

$$v_{gs} = i_{in}\frac{X_{gd} X_{C1,Cgs}}{X_{gd} + X_{C1,Cgs} + X_{C2,Cds}}. \tag{6}$$

Now by substituting v_{gs} from (6) into (5) we obtain

$$v_{in} = i_{in}\frac{X_{gd}\left(X_{C1,Cgs}+X_{C2,Cds}\right)}{X_{gd}+X_{C1,Cgs}+X_{C2,Cds}} + i_{in}g_m\frac{X_{gd}X_{C1,Cgs}X_{C2,Cds}}{X_{gd}+X_{C1,Cgs}+X_{C2,Cds}}. \quad (7)$$

Taking the ratio of v_{in} to i_{in} in (7) then yields

$$Z_{in} = \frac{X_{gd}}{X_{gd}+X_{C1,Cgs}+X_{C2,Cds}}\left(X_{C1,Cgs}+X_{C2,Cds}+g_m X_{C1,Cgs}X_{C2,Cds}\right). \quad (8)$$

Since $X_{gd} = 1/j\omega C_{gd}$, $X_{C1,Cgs} = 1/j\omega\left(C_1+C_{gs}\right)$ and $X_{C2,Cds} = 1/j\omega\left(C_2+C_{ds}\right)$, then we have from (8):

$$Z_{in} = \frac{1}{1+\frac{C_{gd}}{C_1+C_{gs}}+\frac{C_{gd}}{C_2+C_{ds}}}\left(\frac{1}{j\omega C_S}-\frac{g_m}{\omega^2\left(C_1+C_{gs}\right)\left(C_2+C_{ds}\right)}\right), \quad (9)$$

where $C_S = \left(C_1+C_{gs}\right)\left(C_2+C_{ds}\right)/\left(C_1+C_{gs}+C_2+C_{ds}\right)$.

From (9) follows that the input impedance of the circuit shown in fig. 5 is represented by a series connection of a negative resistance

$$r_{neg} = -g_m\Big/\left[\omega^2\left(C_1+C_{gs}\right)\left(C_2+C_{ds}\right)\left(1+\frac{C_{gd}}{C_1+C_{gs}}+\frac{C_{gd}}{C_2+C_{ds}}\right)\right], \quad (10)$$

with a capacitance

$$C_{SP} = C_S\left(1+\frac{C_{gd}}{C_1+C_{gs}}+\frac{C_{gd}}{C_2+C_{ds}}\right). \quad (11)$$

It should be noted that with $C_{gs} = C_{gd} = C_{ds} = 0$, eq. (10) is reduced to a well-known expression [3], [9]

$$r_{neg} = -g_m/\omega^2 C_1 C_2 .$$

Connecting a coil L with the capacitor C_0 and a series total loss resistance r_t to the input impedance Z_{in} we obtain a series equivalent circuit of the Clapp oscillator shown in fig. 6 (*a*).

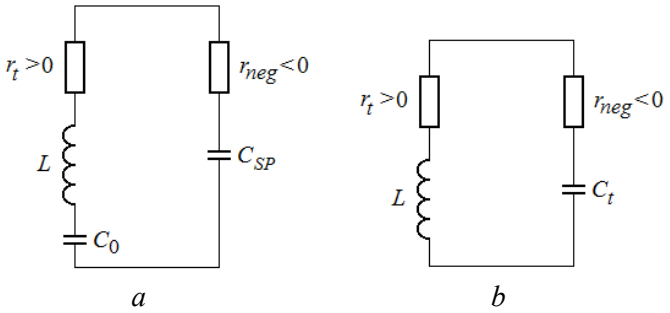

a *b*

Fig. 6. Series equivalent circuit of the Clapp (*a*) and Colpitts (*b*) oscillator

As seen from fig. 6(*a*), the total tank circuit capacitance is given by

$$C_t = \frac{0{,}5C_V C_S\left(1+\frac{C_{gd}}{C_1+C_{gs}}+\frac{C_{gd}}{C_2+C_{ds}}\right)}{0{,}5C_V + C_S\left(1+\frac{C_{gd}}{C_1+C_{gs}}+\frac{C_{gd}}{C_2+C_{ds}}\right)}; \quad (12)$$

Substituting C_t from (12) into the frequency setting equation

$$\omega^2 = 1/LC_t\,, \tag{13}$$

gives

$$\omega^2 = \left[\frac{0,5LC_VC_S\left(1+\dfrac{C_{gd}}{C_1+C_{gs}}+\dfrac{C_{gd}}{C_2+C_{ds}}\right)}{0,5C_V+C_S\left(1+\dfrac{C_{gd}}{C_1+C_{gs}}+\dfrac{C_{gd}}{C_2+C_{ds}}\right)}\right]^{-1}. \tag{14}$$

After substituting ω^2 from (14) to (10), the final expression for r_{neg} can be represented as

$$r_{neg} = \frac{-g_mL}{\left(C_1+C_{gs}+C_2+C_{ds}\right)\left[1+2\dfrac{C_S}{C_V}\left(1+\dfrac{C_{gd}}{C_1+C_{gs}}+\dfrac{C_{gd}}{C_2+C_{ds}}\right)\right]}. \tag{15}$$

From (15) follows that r_{neg} depends on the transistor parasitic capacitances and ratio C_S/C_V. As seen, the greater is ratio C_S/C_V the less will be $|r_{neg}|$. Figure 7 illustrates the dependence of $|r_{neg}|$ on the ratio C_S/C_V calculated with $g_m = 3\text{mS}$, $L = 100\text{nH}$, $C_1 = C_2 = 20\text{pF}$, $C_{gs} = C_{gd} = 2\text{pF}$, and $C_{ds} = 0,25\text{pF}$.

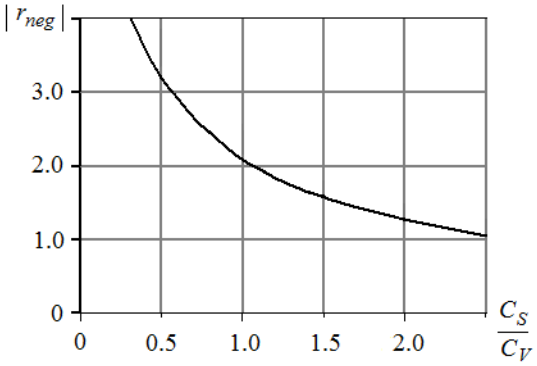

Fig. 7. Dependence of $|r_{neg}|$ on the ratio C_S/C_V

As it could be observed in fig. 7, big ratios of C_S to C_V result in small magnitude of r_{neg}. This impedes the start-up for the Clapp VCO.

Figure 6 (*b*) shows the series equivalent circuit of the Colpitts oscillator. For this circuit the negative resistance and total tank circuit capacitance are determined as follows:

$$r_{neg} = -g_m \Big/ \left[\omega^2\left(C_V+C_{gs}\right)\left(C_V+C_{ds}\right)\left(1+\frac{C_{gd}}{C_V+C_{gs}}+\frac{C_{gd}}{C_V+C_{ds}}\right)\right]; \tag{16}$$

$$C_t = \frac{\left(C_V+C_{gs}\right)\left(C_V+C_{ds}\right)}{2C_V+C_{gs}+C_{ds}}\left(1+\frac{C_{gd}}{C_V+C_{gs}}+\frac{C_{gd}}{C_V+C_{ds}}\right). \tag{17}$$

By substituting (17) into (13), the oscillation frequency is found to be

$$\omega^2 = \left(L\frac{\left(C_V+C_{gs}\right)\left(C_V+C_{ds}\right)}{2C_V+C_{gs}+C_{ds}}\left(1+\frac{C_{gd}}{C_V+C_{gs}}+\frac{C_{gd}}{C_V+C_{ds}}\right)\right)^{-1} \tag{18}$$

Substituting (18) into (16) then yields

$$r_{neg} = -\frac{g_m L}{2C_V + C_{gs} + C_{ds}}. \tag{19}$$

According to (19), the negative resistance is inversely proportional to C_V. Moreover, for the Colpitts VCO resistance r_{neg} does not depend on parasitic capacitance C_{gd}, but it depends on C_{gs} and C_{ds}, which reduce the magnitude of r_{neg}.

The dependence of $|r_{neg}|$ on the value of varactor capacitance C_V for the Clapp and Colpitts VCOs is illustrated in fig. 8 (*a*) and (*b*) respectively for the same data as in fig. 7.

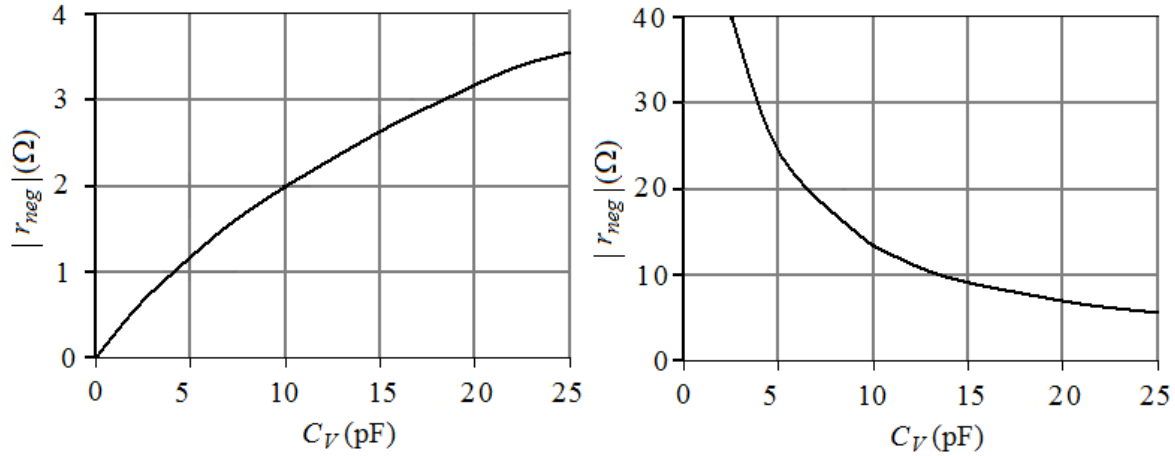

a *b*

Fig. 8. Dependence of $|r_{neg}|$ on the varactor capacitance value C_V for Clapp (*a*) and Colpitts (*b*) VCO

Comparing the plots shown in fig.8, one can conclude that the Clapp VCO has an inherently more difficult start-up condition than the Colpitts VCO because $|r_{neg}|_{Colpitts} > |r_{neg}|_{Clapp}$. Therefore, a higher small-signal transconductance and greater power consumption are required for the Clapp oscillator to achieve reliable start-up.

Referring to the equivalent circuits of fig. 6 we find that to enable oscillation, the negative small-signal resistance r_{neg} added by the transistor should overcome the losses represented by r_t. Taking into account that any VCO operates in a fixed frequency range where the varactor capacitance changes from $C_{V\min}$ to $C_{V\max}$, the guaranteed start-up condition for both VCOs in terms of the series equivalent circuits of fig. 6 is given by

$$|r_{neg}|_{\min} > r_t, \tag{20}$$

where $|r_{neg}|_{\min}$ is the minimum magnitude of the negative resistance in the selected frequency range. As seen from Fig. 8, $|r_{neg}|_{\min}$ corresponds to $C_{V\min}$ for the Clapp VCO and to $C_{V\max}$ for the Colpitts VCO.

In the steady state a nonlinear mechanism reduces g_m to a large-signal transconductance G_m $(G_m < g_m)$ so that at any oscillation frequency $|r_{neg}| = r_t$.

For both Clapp and Colpitts VCOs the total series loss resistance r_t is found as

$$r_t = r_L + 2r_V$$

where r_L and r_V are, respectively, the coil and the varactor diode series resistance.

The start-up condition for both VCOs can also be represented in terms of the parallel equivalent circuit shown in Fig. 3. Indeed, performing a series to parallel transformation the negative resistance loading the parallel tank circuit is determined as

$$R_{neg} = -\left(2C_V + C_{gs} + C_{ds}\right)^2 \Bigg/ \left[g_m \left(C_V + C_{gs}\right)\left(C_V + C_{ds}\right)\left(1 + \frac{C_{gd}}{C_V + C_{gs}} + \frac{C_{gd}}{C_V + C_{ds}}\right)\right], \qquad (21)$$

for the Colpitts VCO. Analogically, the parallel negative resistance R_{neg} can be derived for the Clapp VCO.

The equivalent parallel resistance of the tank for the Colpitts VCO topology can easily be found as

$$R_P = \frac{L}{r_t \dfrac{\left(C_V + C_{gs}\right)\left(C_V + C_{ds}\right)}{2C_V + C_{gs} + C_{ds}}\left(1 + \dfrac{C_{gd}}{C_V + C_{gs}} + \dfrac{C_{gd}}{C_V + C_{ds}}\right)}.$$

It is evident from the above given theoretical analysis that the VCO performance characteristics are dependent on the transistor parasitic capacitances C_{gs}, C_{gd} and C_{ds}. For example, assuming $g_m = 3\text{mS}$, $C_V = 10\text{pF}, C_{gs} = C_{gd} = 2\text{pF}$, and $C_{ds} = 0,25\text{pF}$ one can calculate from (21) that $R_{neg} = -985\Omega$, while for the ideal VCO model we have $R_{neg} = -4/g_m = -1333\Omega$. Thus neglecting the transistor parasitic capacitances a 35 % error is introduced in estimation of R_{neg}. Therefore, at high frequencies the parasitic capacitances should be taken into account.

Simulation results. To confirm the validity of theoretical modeling, we compare the results of calculations and SPICE simulations, performed with MULTISIM, for the Colpitts and Clapp oscillator circuits shown in fig. 2. A JFET BF245B was selected for both oscillators with pinch-off voltage $V_P = -2,31\text{V}$ and $I_{DSS} = 6,2\text{mA}$, where I_{DSS} is the transistor drain-source current in saturation with zero gate-source voltage. For both oscillators the coil inductance was chosen to be 100nH and $V_{DD} = 5\text{V}$. The source impedance circuit for both oscillators is shown in fig. 9.

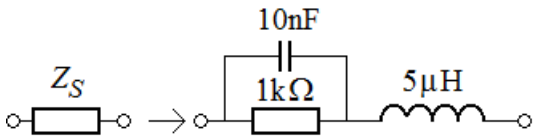

Fig. 9. The source impedance circuit

The capacitances were selected as follows: $C_{V1} = C_{V2} = C_V = 10\text{pF}$ – for the Colpitts oscillator and $C_1 = C_2 = 40\text{pF}$, $C_0 = 9\text{pF}$ – for the Clapp oscillator. The dc value of the drain-source current was calculated from the Shockley equation resulting in $I_{DQ} = 1,27\text{mA}$. Using well-known equations and SPICE file of JFET BF245B the other parameters were calculated giving the following results: $g_m = 2,43\text{mS}$, $C_{gs} = 1,33\text{pF}$, $C_{gd} = 0,90\text{pF}$ and $C_{ds} \approx 0$. The simulated maximum values of r_t providing sustained oscillations at $f \approx 200,2\text{MHz}$ and calculated values of r_{neg} for both oscillators are given in table.

Simulated and theoretical results

Simulated value $r_{t\max}$ (Ω)		Theoretical value r_{neg} (Ω)	
Colpitts oscillator	Clapp oscillator	Colpitts oscillator	Clapp oscillator
9,3Ω	0,5	-11,4	-0,54

As seen from table 1, the Colpitts oscillator can provide sustained oscillations with maximum total loss resistance of 9,3Ω, while the Clapp oscillator can do the same with only $r_{t\max}$ =0,5Ω. Thus the Colpitts oscillator has an inherently more powerful starting-up than the Clapp oscillator. It should be noted that for both oscillators $|r_{neg}| > r_{t\max}$, which proves the validity of the start-up condition (20).

The time required to reach a steady-state oscillation level (τ_{ss}) is an important performance characteristic for any oscillator. Figure 10 illustrates the Colpitts (*a*) and Clapp (*b*) oscillator starting waveform for case when $r_t = 0,25\Omega$. As seen, the output voltage amplitude is within 3 dB of the steady-state output level in approximately 350 nS and 5,8 μS correspondingly for the Colpitts and Clapp oscillator. The fact that $(\tau_{ss})_{Colpitts} << (\tau_{ss})_{Clapp}$ once again demonstrates that the Clapp oscillator has less powerful start-up than the Colpitts oscillator. Therefore, the Clapp oscillator can only be designed with a high-*Q* inductors and varactors rising in price of fabricated VCOs. While the Colpitts oscillator can be designed with low-*Q* and low-cost components. This is very important advantage of the Colpitts VCO arising from the results of this paper.

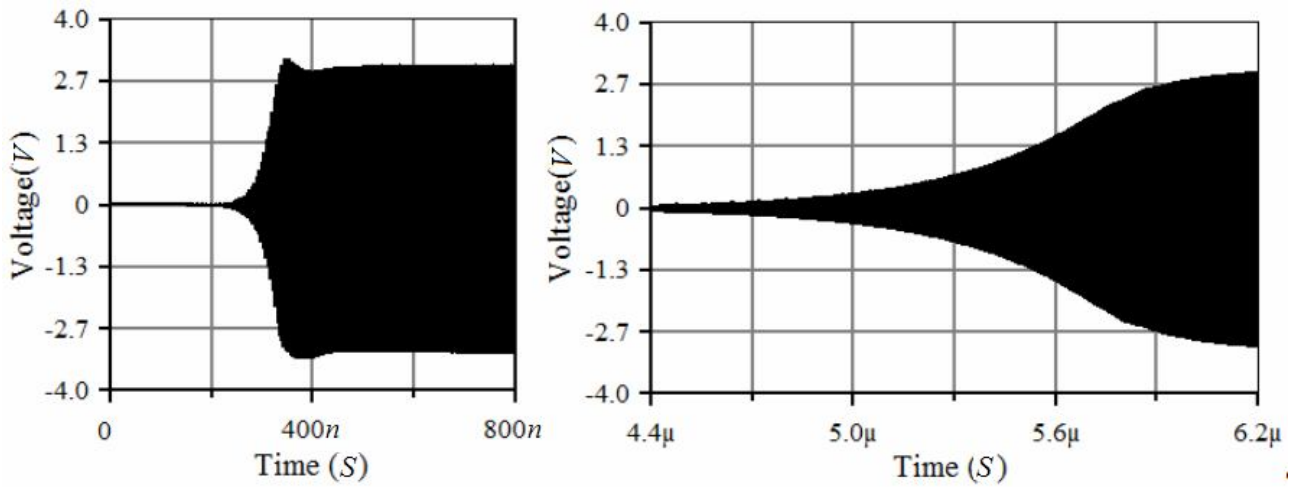

a *b*

Fig. 10. Starting waveform: *a* – Colpitts oscillator; *b* – Clapp oscillator

Conclusions. Unlike the traditional approach of modeling the Colpitts and Clapp oscillators with neglected parasitic elements, the proposed mathematical model takes into consideration the transistor terminal capacitances as well. For both series and parallel equivalent circuits of the oscillators, the analytical expressions have been derived for precise prediction of the oscillation frequency and small-signal negative resistance. These expressions have been verified by SPICE simulations. For the first time it was shown that the Colpitts oscillator has inherently more powerful start-up condition than the Clapp oscillator. From this fact follows that the Colpitts voltage-controlled oscillators can be designed with low-cost inductors and varactors, while the Clapp oscillators require more expensive components.

References

1. *Rhea R. W.* Oscillator design and computer simulation. – 2nd ed. – Atlanta: Noble, – 2008. – 303 p.
2. *Leenarts D., Van der Tang J., Vaucher C.* Circuit design for RF transceivers. – Boston: Kluwer. Academic Publishers, – 2001. – 311 p.
3. *Razavi B.* Design of Analog CMOS Integrated Circuits. – Boston: McGraw–Hill, 2001. – 684 p.
4. *Van der Tang J., Kasperkovitz D., Van Roermund A.* High-frequency oscillator design for integrated transceivers. – London: Springer: 2003. – 343 p.
5. *Aparicio R., et al.* A Noise-Shifting Differential Colpitts VCO // IEEE J. Solid-State Circuits. – 2002. – Vol. 37. – P. 1728 – 1736.
6. *Hegazi E., Rael J., Abidi A.* The designer`s guide to high purity oscillators. – London: Springer, – 2004. – 204 p.
7. *Odyniec M.* RF and microwave oscillator design. – Artech House Publishers, – 2002. – 416 p.
8. Trimless IF VCO: Part 1: Design considerations // Application note 2032. – http: // www.maxim-ic.com/an 2032.
9. *O`Connor C.* Develop a trimless voltage-controlled oscillators // Microwaves and RF. – January 2000. – P. 94 – 105.

В. В. Уланский, М. Ф. Абусаид, И. А. Мачалин

Математическое моделирование генераторов, управляемых напряжением с топологией Колпица и Клапа

Представлено аналитическое моделирование генераторов управляемых напряжением с топологией Колпица и Клапа, из которого выведены более точные уравнения для расчета частоты генерируемых колебаний и отрицательного сопротивления в режиме малого сигнала. Моделирование выполнено с учетом паразитных емкостей полевого транзистора. Дается сравнение условий самовозбуждения для генераторов Колпица и Клапа, подтвержденное SPICE имитацией. Приведенные уравнения гарантируют более точное моделирование, проектирование и изготовление генераторов управляемых напряжением с топологией Колпица и Клапа.

В. В. Уланський, М. Ф. Абусаід, І. О. Мачалін

Математичне моделювання генераторів, керованих напругою з топологією Колпіця та Клапа

Подано аналітичне моделювання генераторів керованих напругою з топологією Колпиця та Клапа, з якого виведено більш точні рівняння для розрахунку частоти генерованих коливань та негативного опору в режимі малого сигналу. Моделювання виконано з урахуванням паразитних ємностей польового транзистора. Подано порівняння умов самозбудження для генераторів Колпіця та Клапа, підтверджуване SPICE імітацією. Наведені рівняння гарантують більш точне моделювання, проєктування та виготовлення генераторів керованих напругою з топологією Колпіця та Клапа.